Fusion Technology

ISSN: 0748-1896 (Print) Journal homepage: www.tandfonline.com/journals/ufst19

Magnetized Target Fusion: An Overview

Ronald C. Kirkpatrick, Irvin R. Lindemuth & Marjorie S. Ward

To cite this article: Ronald C. Kirkpatrick, Irvin R. Lindemuth & Marjorie S. Ward (1995) Magnetized Target Fusion: An Overview, Fusion Technology, 27:3, 201-214, DOI: 10.13182/FST95-A30382

To link to this article: https://doi.org/10.13182/FST95-A30382

Published online: 09 May 2017.

MAGNETIZED TARGET FUSION: AN OVERVIEW

SPHERICAL PLASMA CONFIGURATIONS

KEYWORDS: *magnetized target fusion, pulsed power, neutron production*

RONALD C. KIRKPATRICK, IRVIN R. LINDEMUTH, and MARJORIE S. WARD
Los Alamos National Laboratory, Los Alamos, New Mexico 87545

Received January 3, 1994
Accepted for Publication January 7, 1994

The magnetized target fusion (MTF) concept is explained, and the underlying principles are discussed. The necessity of creating a target plasma and the advantage of decoupling its creation from the implosion used to achieve fusion ignition are explained. The Sandia National Laboratories Φ-target experiments is one concrete example of the MTF concept, but other experiments have involved some elements of MTF. Lindl-Widner diagrams are used to elucidate the parameter space available to MTF and the physics of MTF ignition. Magnetized target fusion has both limitations and advantages relative to inertial confinement fusion. The chief advantage is that the driver for an MTF target can be orders of magnitude less powerful and intense than what is required for other inertial fusion approaches. A number of critical issues challenge the practical realization of MTF. Past experience, critical issues, and potential integral MTF experiments are discussed.

I. INTRODUCTION

The use of a magnetic field to inhibit thermal conduction is not a new idea. The idea seems to have originated at Los Alamos National Laboratory (LANL) in about 1945, possibly with Landshoff[1] or Teller, as evidenced at that time in the records of a series of lectures by Fermi, and has been revisited several times. Each time there has been added insight not only into the various physics processes but also into their interplay. In addition, there has been experimental progress over as many as three decades to the point that some who are sufficiently familiar with magnetized target fusion (MTF) think that an irrefutable proof-of-principle experiment is now possible.

Magnetized target fusion consists of the hydrodynamic compression of a wall-confined, hot, magnetized deuterium-tritium (D-T) plasma to ignition conditions. The most notable MTF experiments were the Φ-target experiments done on an electron-beam machine at Sandia National Laboratories[2] (SNL), but imploding liner fusion schemes and some impact fusion schemes share the same principles as MTF. Magnetized target fusion takes advantage of two benefits of a magnetic field in a plasma: reduction of the thermal conductivity[1] and potentially the enhancement of the charged-particle reaction product energy deposition in the plasma.[3] The reduction of thermal conductivity by the magnetic field should be classical (Spitzer rather than Bohm), and even in the absence of self-heating (i.e., no D-T alpha-particle energy deposition), parameter studies have shown that targets with gains as high as ten are possible.[4] Synchrotron radiation is an undesired consequence of the field, but it is unimportant for MTF (Ref. 5). While the field strength is sufficient to achieve the aforementioned desired effects, the plasma is still very high beta ($\beta \gg 1$, where β is the particle-to-magnetic-pressure ratio), so that the dynamics are determined by the gas pressure, not the field pressure. To reduce the radiative energy loss from the plasma so that conduction is the major energy loss mechanism (even when suppressed by the magnetic field), we make the initial density of the D-T much lower than that used for inertial confinement fusion (ICF). This makes the targets larger, and the reduced losses allow a lower compression rate, so that the implosion time can be long and the necessary power and intensity on target can be very low. The parameter space for MTF is intermediate in density and timescales between those of ICF and magnetic confinement for fusion energy (MFE). The energy required for ignition of a magnetized target is comparable to that for an ICF target with the same mass of D-T, but the power and power density required are much less, so that some

existing pulsed power machines should be capable of igniting an MTF target. The ignition of a cold fuel layer by a burning central magnetized fuel should significantly increase the gain of a magnetized fuel target.[6]

A note on the acronym MTF is necessary. This concept has been referred to as magnetized fuel, magnetized fuel ICF, and the fast liner program at LANL. Elsewhere it has had other names. The commonality among the various incarnations of this concept is the need for a preheated, magnetized plasma in which the magnetic field inhibits thermal conduction while the plasma is subsequently imploded to achieve fusion temperatures.

This paper is not intended to be a comprehensive review of MTF. Rather, it is an overview of MTF from a theorist's viewpoint. We discuss some elementary analyses, parameter studies, and computer simulations, as well as a few relevant experiments.

II. UNDERLYING PRINCIPLES

Magnetized target fusion falls in a region of parameter space that is intermediate between ICF and MFE; both magnetic field and implosion are necessary for reaching fusion conditions. It involves utilizing a magnetic field to reduce energy losses from the plasma during the course of the implosion and to enhance fusion energy deposition at the time of ignition. Magnetized target fusion is not just a variation of ICF or a variation of magnetic confinement fusion. The role of the magnetic field is to inhibit thermal conduction and to enhance fusion reaction product energy deposition within the target plasma, but not to confine the plasma. There is no attempt to magnetically confine the fusion plasma, and although we have looked at the effect of polarization of the fusion nuclei, we do not usually include this effect in our calculations because it makes a relatively small improvement. The results of survey calculations[4] published in 1983 suggested that significant gain could be obtained even in the absence of ignition, but clearly, self-heating would substantially increase gain.

The underlying principles of MTF are

1. reduction of thermal conduction by the application of a strong magnetic field
2. establishment of an elevated initial fuel adiabat by a preheat mechanism that can be the same as or different from the magnetization method
3. operation at relatively low density to reduce radiative losses
4. stabilization of the plasma by the inertia of an imploded shell that dynamically supports, compresses, and heats the high-beta, magnetized D-T plasma inside
5. compression of the field together with the plasma, which may lead to enhanced D-T alpha-particle energy deposition.

III. TARGET PLASMA

Magnetized target fusion requires an initially hot, magnetized plasma (e.g., ~50 eV and ~50 kG) inside a shell that can be imploded to compress and heat the plasma to ignition conditions. To trap the initial magnetic field during the implosion, either the plasma or the pusher must have high electrical conductivity. While a strong field can greatly reduce transverse thermal conductivity, it can reduce the transverse electrical conductivity by only a factor of 2 at most. There is a relation between the electrical and thermal conductivity and the thermoelectric and Nernst coefficients for a plasma. All the relevant terms are included in the detailed simulation codes we have used, but in the simplified models that we have used for survey calculations, we have included only those terms that appear to be important for MTF. For example, the Nernst effect is very small for MTF.

A temperature of 50 eV makes the plasma sufficiently conductive to reduce the diffusion coefficient for the magnetic field and effectively freeze the field to the plasma during the implosion phase. At sufficiently low density, an initial field of 50 kG provides a cyclotron frequency times collision time product $\omega\tau > 1$, so that the thermal conductivity is reduced to allow slower implosions to drive the target to fusion temperatures.

The initial B field trapped in the imploding target is compressed and continues to ever more strongly reduce thermal conductivity. Both $\omega\tau$ and plasma-to-field-pressure ratio β increase as the implosion proceeds. The field can even become sufficiently large (providing a field times radius product $BR > 0.3$ MG·cm) to enhance energy deposition (i.e., the thermonuclear self-heating) by the charged fusion reaction products. The complex trajectory in a strong field increases the path length in the fuel to a substantial fraction of the D-T alpha-particle range.

IV. IGNITION AND BURN

Two steps are needed for MTF: (a) the creation of a target plasma and (b) compression of the target plasma to fusion temperatures.

For ICF, an unmagnetized target plasma is created by a strong shock that enters the cold D-T from the pusher at the beginning of the implosion, thus restricting the character of the implosion capable of igniting the D-T. For MTF, the target plasma creation process is decoupled from the implosion, thereby providing more freedom in the choice of implosion systems.

If the physics processes are in accord with our current understanding, MTF ignition can occur when very low implosion velocities for plasmas with very low ρR and densities (by ICF standards) are used. This is possible because the major heat loss mechanism, thermal conduction, is suppressed by megagauss fields, and the D-T alpha particles are partially trapped within the plasma.

The region of parameter space where MTF operates is illustrated in Fig. 1, which shows the regions in the areal density, temperature ($\rho R, T$) plane where the fusion processes dominate over the plasma energy losses. These are the boundaries for bootstrapping burn ($dT/dt > 0$) in the absence of external support (pusher $v = 0$) and are marked for ICF and MTF. We call Fig. 1 a Lindl-Widner diagram.[7] Note that MTF ignition occurs at much lower values of PR (proportional to the product of ρR and T) than for ICF and that because the energy needed to ignite the D-T goes as mc_vT, the pressure at the time of ignition is also lower than for ICF.

Because MTF ignition occurs when the plasma density is on the order of only 1 g/cm^3, the burn time is relatively long. Also, the ρR is very low, and the ignition temperature is only moderately higher than for ICF, so that the pressure times radius parameter PR needed for MTF ignition is orders of magnitude lower than for ICF. As shown in Sec. XII, the value of PR required for ignition enters into the equation for the minimum implosion energy necessary for fusion ignition.

V. SNL Φ-TARGET

The SNL Φ-target provides a concrete example of a magnetized target. A schematic illustration of the Φ-target is shown in Fig. 2. In about 1977, Widner, Chang, and others at SNL added a small collector plate to an electron-beam target.[2] The collector plate was intended to intercept the nonrelativistic prepulse from their machine, and it created an electrical discharge through the target. This magnetized the gas inside and ohmically heated it to create a target plasma. The collector plate was transparent to the relativistic electrons, which reflexed several times through the target, providing a fairly symmetric implosion of the inner aspect of the pusher to compress the target plasma. No funding was committed to this work, and only the available diagnostics were used. Because the appropriate diagnostics were not available, no direct compression measurements were done.

Sandia National Laboratories obtained 5 to 25 × 10^6 neutrons from 8 of 15 complete targets and fielded 24 null experiments. The null experiments used targets with holes or lumps on the microballoon, or without a collector. Some targets had CD_2 fibers as a plasma source, and others had a deuterium fill. Lindemuth and Widner[8] modeled one of the experiments with a deuterium fill using both one- and two-dimensional codes. On that basis, they provided the following characterization.

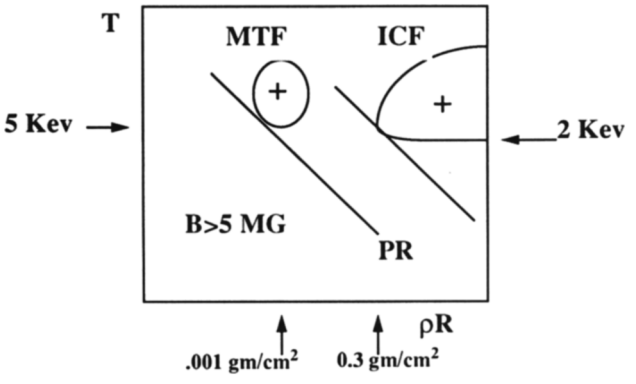

Fig. 1. The regions in the ($\rho R, T$) parameter space where ICF and MTF operate. These are the boundaries for bootstrapping burn ($dT/dt > 0$) in the absence of external support (pusher $v = 0$).

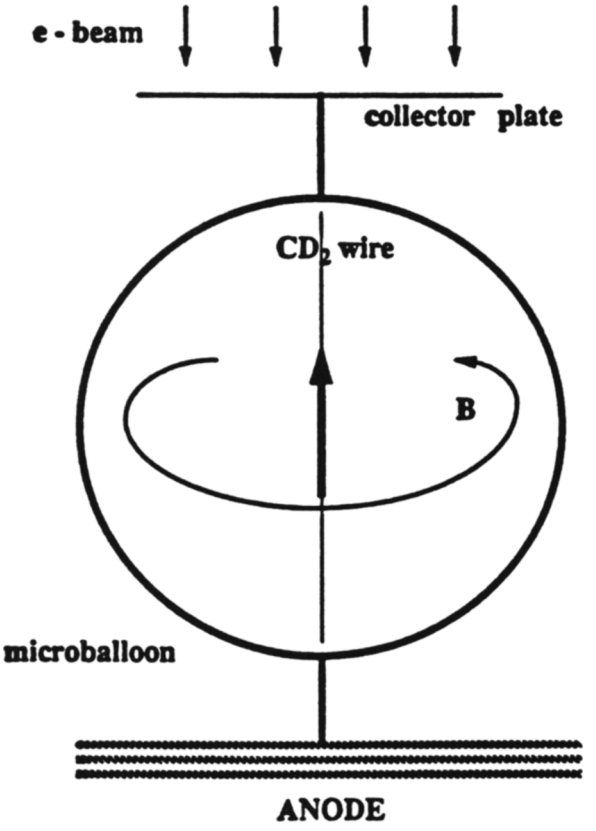

Fig. 2. A schematic illustration of the Φ-target used by Widner, Chang, and others at SNL for electron-beam experiments in 1977.

The inferred conditions after a 1-μs and 12-kA-(nonrelativistic) prepulse were 2 mg/cm^3 density, 20-eV temperature, and 10-kG field. The main (relativistic) pulse was 1 MeV, 200 kA, 0.1 μs, and 4 kJ. The experimental results were 5 to 25 $\times$ 10^6 neutrons for 8 of 15 complete targets and none for 24 null targets (with holes and lumps, or no collector). The inferred conditions at turnaround were >20 convergence, >400 eV, ~1-MG field, and $\omega\tau \sim 5$.

According to survey calculations done a few years later,[4] the Φ-targets actually operated in a region of minimized neutron yield. Apparently, whether the initial deuterium density had been raised or lowered, the neutron yield would have been greater.

VI. LINDL-WIDNER DIAGRAMS

Both Lindl at Lawrence Livermore National Laboratory (LLNL) and Widner when at SNL used a temperature ρR phase plane in which temperature rate or net power density contours were used to illustrate the interplay of physics processes for D-T ignition. Reference 7 presents an excellent discussion of the fusion ignition process for ICF.

All historical definitions of fusion ignition are based on the concept of a threshold that is a dividing line between strikingly different behaviors of the thermonuclear plasma. Familiar examples of thermochemical ignition are striking a match and the combustion that takes place in a diesel engine. Thermonuclear ignition is similar. Prior to ignition in ICF, the plasma state is determined mainly by the hydrodynamics of the implosion, but following ignition, self-sustaining thermonuclear burn occurs and continues despite the expansion cooling that ensues. A comparison of the relevant heating and cooling mechanisms in the D-T plasma of an ICF target shows that ignition conditions can occur in a parameter space that is characterized by a minimum ρR and a minimum temperature, the ignition temperature.

The net power P_{net} due to heating by compression and fusion and cooling by expansion, radiation, and conduction is

$$P_{net} = PdV/dt + Qn^2\langle\sigma v\rangle V - brems - Compton - A\kappa\nabla T \ , \quad (1)$$

where

P = pressure

V = plasma volume

Q = reaction energy

n = density

$\langle\sigma v\rangle$ = velocity-averaged cross section for the fusion reaction

A = interface area

κ = thermal conductivity

T = temperature.

The terms in Eq. (1) are dependent on temperature and density (or ρR) in the plasma, as well as the target radius and implosion velocity. We have not given the full expressions for the bremsstrahlung and Compton cooling terms but have merely indicated their presence. Lindl[7] and Kilcrease and Kirkpatrick[5] have provided different forms of these terms, but the resulting Lindl-Widner diagrams are the same for ICF and MTF.

As an implosion proceeds, the radius R of the target decreases and is often displayed as an $R(t)$ plot. In addition, one can look at the velocity $v(t)$. For a very energetic implosion created by rapid energy deposition in the pusher, a strong shock is created, which when it emerges from the pusher into the D-T inside suddenly sets the interface in motion and continues toward the center of the target. A rarefaction propagates back into the pusher, which typically results in a pusher velocity that is about double that of the shock that initially moved through the pusher. The shock in the D-T creates a plasma and sets the conditions of temperature and density for the compression that follows. Often this is referred to as the initial adiabat, but actually, the process may be sufficiently dynamic and the implosion so fast that significant convergence occurs before the shock reaches the center. Following convergence of the shock, reflected shocks interact with the incoming flow. In an implosion initiated by a shock, the velocity of the interface suddenly goes from zero to a nearly constant value that persists until the pressure inside builds sufficiently to oppose the implosion. This usually occurs shortly before the maximum compression and the velocity falls rapidly to zero—the occurrence of which is usually referred to as turnaround. Disassembly follows. If ignition does not occur, then the disassembly is similar in character to the implosion, but if ignition does occur, energy from the nuclear reactions is deposited in both the D-T plasma and the pusher so that violent shocks cause very high velocities in the disassembly process.

If the implosion is not very energetic, then weaker shocks are involved. The initial adiabat is lower, and the process is less dynamic, approaching a homogeneous compression. For the purposes of the discussion that follows, we assume that the compression is homogeneous. This is a better assumption for MTF than for ICF and also simplifies the discussion for ICF.

The foregoing description of the implosion can be paralleled in the Lindl-Widner parameter space. This is most easily applied for the case of homogeneous compression. For a given implosion velocity, the $-PdV/dt$ compressional work term modifies the boundaries between the regions of negative and positive P_{net}, connecting the positive equilibration region below the

radiation temperature and the positive fusion region at high temperature and ρR. One can also view the progress of the plasma from some initial low value of ρR and temperature through the Lindl-Widner diagram as a $(\rho R, T)$ trajectory for which both ρR and T are increasing as the result of compression as the implosion proceeds.

Inertial confinement fusion does not take advantage of the benefits that may accrue from using a magnetic field. Inertial confinement fusion is the $B = 0$ case; Fig. 3 shows a Lindl-Widner diagram for this case. Note that there are two regions of positive temperature rate: one for the plasma temperature below the specified radiation temperature (100 eV) and one at temperatures where the fusion reaction cross section is large for D-T. The upper region does not extend below 0.2 g/cm^2 because with $B = 0$, the thermal conduction is too large and the energy deposited in the D-T too low to allow bootstrapping fusion burn. Figure 3 was drawn for a uniform work rate on the D-T (such as occurs in a homogeneous implosion) set to zero, as would be the case at turnaround when the motion of the pusher of an ICF target reverses.

Figure 4 shows that for sufficiently high implosion velocity, the compressional work rate on the D-T plasma is sufficient to overcome the loss mechanisms (bremsstrahlung, conduction, etc.) and allow the positive temperature rate regions at low and high temperature to connect. If the initial temperature and density (or ρR) of the plasma as set by an initial strong shock in the D-T at the outset of the implosion are just right, then the implosion trajectory will extend from the low initial values into the fusion region. With sufficiently strong implosions (i.e., high enough initial velocity and sufficient pusher mass), the trajectory will be nearly adiabatic. In Fig. 4, an adiabat has unity slope. If ignition occurs, as the motion of the pusher reverses, the density begins to decrease, but the fusion energy deposition more than offsets the expansion cooling so that the temperature continues to increase. A hypothetical trajectory is superimposed on Fig. 4.

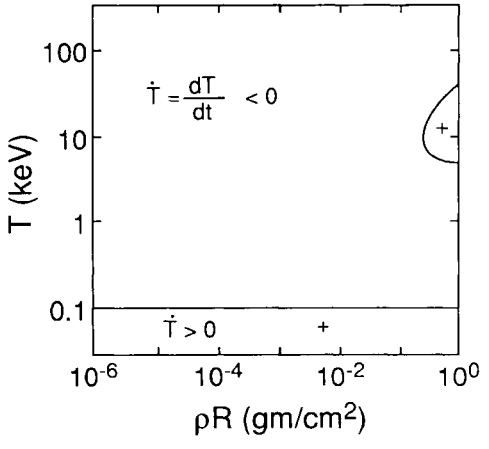

Fig. 3. The Lindl-Widner diagram for the $B = 0$ case. Inertial confinement fusion does not take advantage of the benefits of a magnetic field.

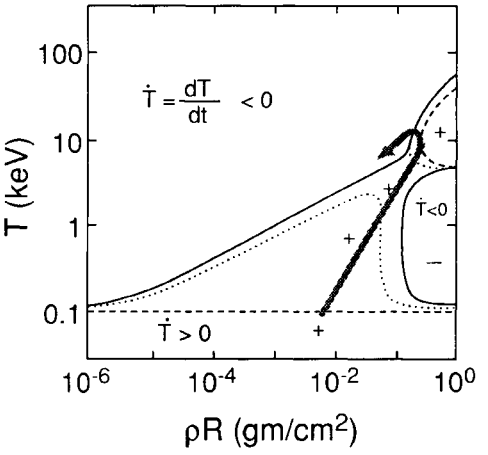

Fig. 4. Lindl-Widner diagram for $B = 0$ with compressional work rate included for $v = 0$, 10, and 20 cm/μs.

VII. PARAMETRIC LINDL-WIDNER DIAGRAMS

Magnetized target fusion seeks to take advantage of the benefits and to endure the penalties of an embedded magnetic field. A comparison of the relevant heating and cooling mechanisms in the presence of a magnetic field shows that ignition conditions can occur in a new parameter space intermediate between, but remote from, both the regime for conventional ICF and the regime of magnetic confinement fusion. The net power due to heating by compression and fusion and cooling by expansion, radiation, and conduction is

$$P_{net} = PdV/dt + Qn^2\langle\sigma v\rangle V - brems - Compton - sync - A\kappa\nabla T \; . \qquad (2)$$

The terms in Eq. (2) are dependent on temperature and density in the plasma as well as the target radius and implosion velocity and the magnetic field in the D-T plasma. The synchrotron cooling term is indicated as *sync* in Eq. (2) and is discussed fully by Kilcrease and Kirkpatrick[5] for MTF.

Figure 5 shows that the Lindl-Widner diagrams can be conveniently overlaid with lines of constant plasma parameters to provide a map for magnetized fuel ignition. The plasma magnetization parameter $\omega\tau$ for the electrons determines the degree to which the electron thermal conductivity is reduced in a plasma. The

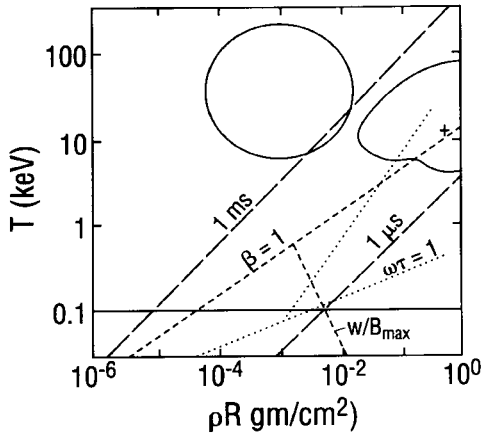

Fig. 5. The Lindl-Widner diagrams overlaid with lines of constant plasma parameters to provide a map for magnetized fuel ignition.

plasma-to-field energy density or pressure ratio β determines the importance of the magnetic field in pushing the plasma around (i.e., the buoyancy of the high field regions). If the plasma has a high β, then the field can only weakly push the plasma around, and the timescale for this process is relatively long. The plasma-to-cyclotron frequency ratio ω_p/ω determines the persistence of plasma fluctuations, which enhance plasma transport. When this ratio is large, the fluctuations do not persist, and Bohm diffusion is not important. The resistive timescale for the plasma is determined by the conductivity of the plasma or the pusher and the inductance of the current paths within the plasma and pusher. Long resistive timescales mean that the magnetic field will be effectively frozen to the plasma and that the two will move together [the ideal magnetohydrodynamic (MHD) case].

In the Lindl-Widner diagrams that follow, we have made the simplifying assumptions that a B_θ field is frozen in the plasma and the plasma undergoes a spherical implosion. Then, B_θ is proportional to ρR (along the horizontal axis of the Lindl-Widner diagram).

For the MTF case ($B > 0$) shown in Fig. 5, the ICF fusion region is significantly enlarged and extended to the left, and a new MTF region appears to the left of it. A (dashed) line of $\beta = 1$ is plotted in Fig. 5. For the MTF region, the plasma pressure dominates over the magnetic field pressure. Note that Fig. 5 is drawn for a target containing 100 μg of D-T at the time of turnaround. Also, the field has been limited to 10 MG, and the dashed line with negative slope shows the effect of this limiting, which occurs at $\sim\rho R = 0.002$ g/cm^2. Note that the details of the target (size, etc.) can cause a shift of these parameter lines in Fig. 5. The dotted line for the cyclotron frequency times collision time product $\omega\tau = 1$ is also overlaid on the Lindl-Widner diagram. As expected, the MTF region lies in the high $\omega\tau$ region, where thermal conduction is strongly inhibited. The intersecting dotted line with steeper slope shows the effect of limiting the field to 10 MG. Two constant resistive timescale lines (long dashes labeled 1 ms and 1 μs) have been added to the diagram. It is apparent that the resistive timescale for the MTF region is long.

VIII. MINIMUM MASS FOR IGNITION

For MTF, we can draw the Lindl-Widner diagram for the case of a given mass of D-T (m) and ratio of the magnetic field (B) to ρR. For the case of $B = 0$, we get the Lindl-Widner diagram for ICF. In this case, the diagram changes little for various D-T masses. Figure 6 shows that for a sufficiently large ratio of $B/\rho R$, the size and the position of the region where MTF ignition can occur depend on the D-T mass for which the diagram is drawn. For D-T mass less than a few micrograms, MTF ignition does not occur for $B < 5$ MG.

Unlike ICF, the fusion region for MTF in the Lindl-Widner diagram is sensitive to the mass of the D-T in the target. This sensitivity just reflects the fact that the additional physical processes involved in MTF do not have the same dependence on density and target radius separately, so the equations do not scale in the simple way with ρR that ICF does. For a target containing 10 μg of D-T, the MTF region is considerably smaller than for 100 μg, and even the ICF region is hardly enlarged at all. However, for 1000 μg, the ICF and MTF regions connect, providing a wide choice of initial values of ρR, hence, target designs, for which ignition can be achieved.

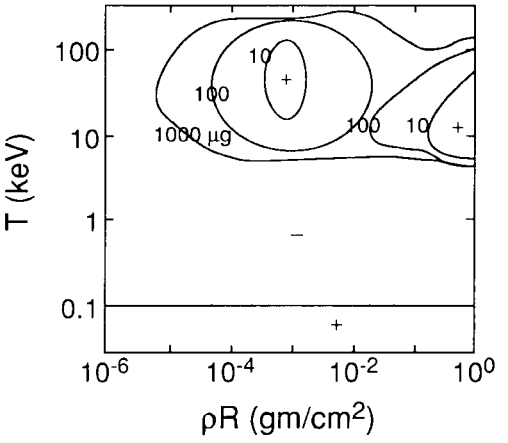

Fig. 6. For a sufficiently large ratio of $B/\rho R$, the size and position of the region where MTF ignition can occur depend on the D-T mass for which the diagram is drawn. Here, $B/\rho R$ is 10000 MG·cm^2/g, and the 10-, 100-, and 1000-μg cases are shown. For D-T mass less than a few micrograms, MTF ignition does not occur for $B < 5$ MG, but for 1000 μg, the ICF and MTF regions merge.

IX. THE PROGRESS OF AN MTF IMPLOSION

As illustrated in Figs. 3 and 4, as the implosion of a plasma progresses, ignition is achieved by providing a rate of work on the plasma sufficient to overpower the various energy loss rates. Initially, the work rate increases as $-3mc_vTv/R$ (for volumetric compression) because the implosion velocity v is only slowly changing at first and R is decreasing. However, as the kinetic energy in the pusher is exchanged for internal energy in the plasma, v must eventually reverse in sign at the time of turnaround, so the work rate must also reverse sign as expansion cooling begins and the plasma does work on the pusher. Thus, a succession of Lindl-Widner diagrams that track a dynamic case should reflect the continually changing energy balance. We wish to follow an MTF implosion to illustrate how MTF ignition differs from ICF ignition (Figs. 3 and 4).

For MTF, the character of the implosion may be very different from that of ICF. The target may use a magnetic implosion, so that the the pusher is accelerated over some period of time and strong shocks are not generated. Still, the $(\rho R, T)$ trajectory is similar to the ICF case for a homogeneous compression.

Figure 7 shows a series of six Lindl-Widner diagrams that trace the implosion of a hypothetical MTF target containing 100 μg. Note that the initial implosion velocity is very low [-0.3 cm/μs (inward) for Fig. 7a]. An adiabatic compression line is drawn from an initial low set of temperature and ρR conditions that must be established when the target plasma is created. The strength of any shock that could pass into the D-T from the pusher for such a low velocity cannot possibly provide a 50-eV plasma. This is why the target plasma preparation is very important to MTF. Some possible approaches to creating a suitable target plasma are discussed in Sec. XIII. Notice that in Fig. 7a, the implosion trajectory must avoid the region of negative temperature rates, which sets a maximum initial ρR that will allow MTF ignition for this particular target. As the pusher continues to slow down (Fig. 7b), the MTF and ICF regions disconnect, and the boundary between the positive and negative temperature rate regions threatens the success of the MTF implosion. When the pusher has nearly turned around (Fig. 7c), the compressional work rate has become very low. At this point, the D-T must have been compressed and heated nearly into the MTF ignition region if ignition is to ensue.

Figure 7d shows the case at turnaround ($v = 0$). If the D-T has attained the conditions represented by the head of the arrow formed by the adiabatic trajectory, then ignition should have occurred, but significant burnup may not be ensured. Expansion cooling shrinks the MTF region for $v = 0.1$ cm/μs in Fig. 7e, but the head of the arrow is still inside the positive temperature rate region. The disassembly of the target continues. Because the head of the trajectory has remained in the positive region, significant bootstrapping should have occurred, and the burn trajectory should curve upward and back to the left as the ρR decreases during disassembly. In Fig. 7f, the thermonuclear energy should have been deposited in the target, and the disassembly velocity could possibly increase to the point that the MTF region disappears altogether. Whether or

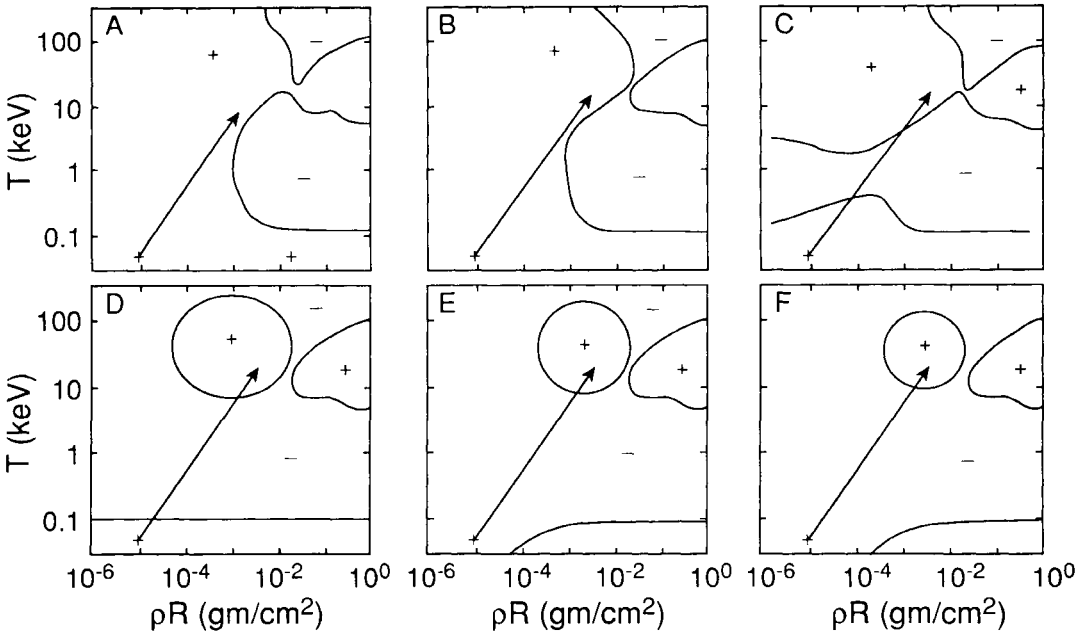

Fig. 7. Hypothetical MTF implosion illustrated by superimposing an implosion $(\rho R, T)$ trajectory on a succession of Lindl-Widner diagrams.

not the MTF region disappears, the expansion will carry the burn trajectory to lower values of ρR, accompanied by decreasing values of B, so that it eventually must leave the MTF region. In addition, depletion and reaction product buildup occur during the thermonuclear burn and change the net heating rate, which should result in more shrinking of the MTF region than these simple Lindl-Widner diagrams (which do not include these effects) show. When the trajectory leaves the MTF (positive temperature rate) region, the temperature must decrease as the target disassembles, so that the D-T reaction rate would rapidly drop. The time spent at high temperature, as well as the reactant depletion, limits the yield and gain of the target.

X. PAST EXPERIENCE

As an example of a magnetized target, we previously discussed the SNL Φ-target. In addition, other concepts can be categorized as MTF, and consequently, various experiments have explored one or more of the physics processes important to MTF. However, none of the experiments, including the SNL Φ-target experiments, has examined all of the underlying principles of MTF listed earlier.

Columbia University researchers in the 1970s addressed the question of thermal conduction inhibition by a magnetic field transverse to the temperature gradient.[9,10] They carried out experiments on a magnetized, shock heated plasma with $\beta \simeq 1$. Feinberg found that in the timescale of the experiment, the heat transport was essentially classical (Spitzer-like) and that at their densities and timescales, turbulence did not play an important role.

At LANL, research on the fast liner concept progressed very rapidly during its brief history.[11,12] Both cylindrical liner implosions and plasma preparation experiments were carried out. The implosions were done with the SCYLLAC capacitor bank and achieved solid liner velocities up to 1 cm/μs with good symmetry. Researchers used a Marshall gun to generate a plasma and inject it into an adjoining cylindrical volume. They obtained a 30-eV plasma with a 10-kG embedded field (lower than desired). The program was terminated prematurely. Jarboe has recently reviewed the fast liner program.[13]

Other experiments may have included one or more elements of MTF, including some in which the effect of magnetization was not considered but was possibly present.[14] The most interesting is the continuing work in Russia. The Russian MAGO experiments are discussed in Sec. XIII.

XI. DEVELOPMENTS SINCE THE EARLY EXPERIMENTS

Since the major experimental results in the United States, that is, the Φ-target and fast liner work, progress has been mainly theoretical and computational. The analysis of the Φ-target experiments by Lindemuth and Widner provided the theoretical and computational underpinning that was needed for a more confident understanding of the results,[8] and survey calculations elucidated the parameter space for MTF (Ref. 4).

More recently, one-dimensional LASNEX calculations have suggested that MTF ignition can occur.[15] These idealized calculations assumed that a spherical target contained 804 μg of D-T at 50 eV with a 30-kG embedded magnetic field. An initial velocity of 1.6 cm/μs was used. At the time the calculation was terminated because of excessive time-step restriction, ~3% burnup had occurred. The LASNEX code has limited magnetic field physics, and is probably inadequate for the design of a small MTF target that reaches a BR of only 0.3 MG·cm. The question of ignition of a cold fuel layer has also been examined.[6,16] It is possible to ignite a cold (frozen D-T) fuel layer from the hot, burning magnetized fuel. Only partial burnup of a cold fuel layer could substantially increase the target gain.

We have determined the minimum energy required for MTF ignition. Unlike ICF, at least a few micrograms of D-T is necessary for MTF ignition. The exact amount depends of the maximum field that can be achieved in the implosion. This is discussed more extensively in Sec. XII.

We now believe that we have a firm basis for claiming that magnetized fuel should operate in the classical regime for reduction of thermal conductivity by the B field. Dawson et al.[17] performed three-dimensional particle simulations that showed that for the plasma-to-cyclotron frequency ratio much greater than unity, plasma fluctuations do not persist sufficiently long for the associated electric fields to cause a net $E \times B$ drift that is at the heart of Bohm diffusion. For magnetized plasmas of interest to MTF, the frequency ratio is very large, >20, so that one would expect that the reduction of thermal conductivity in an MTF plasma should go as B^{-2}. That means that Bohm diffusion should not be important for MTF. There could still be other processes that cause the reduction of thermal conduction to deviate from the classical (Spitzer) behavior, but it appears that Bohm diffusion due to thermal plasma fluctuations can be ruled out.

XII. MINIMUM ENERGY FOR MTF IGNITION

Figure 8 shows the regions in a Lindl-Widner diagram where ICF and MTF operate. As noted previously, the Lindl-Widner diagram for MTF depends on the mass and field to ρR ratio for which the diagram was constructed. This means that the position of the MTF ignition region in the Lindl-Widner diagram may vary from one figure to the next. There are the usual ICF ignition region and a second ignition island at very low ρR due to the presence of a 3.3-MG magnetic field

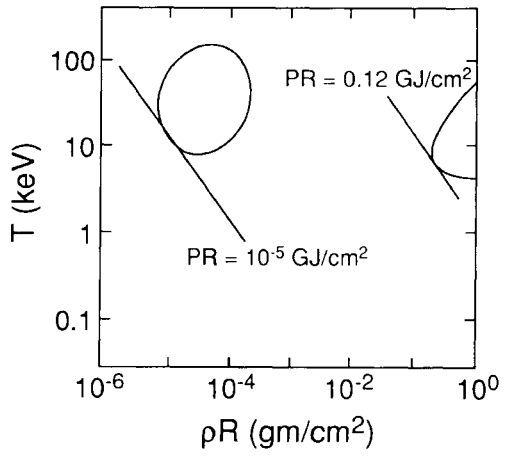

Fig. 8. The minimum pressure times radius parameter *PR* needed for ignition.

in this target with 13.6 μg of D-T. This particular diagram has lines of constant pressure times radius (*PR* is proportional to *T* times ρR) marked to show the minimum possible values that will allow ignition for ICF and MTF. For MTF, the value of this parameter required for ignition can be orders of magnitude lower than for ICF. The parameter of importance for the hydrodynamic compression by a confining shell (a pusher) is *PR*.

Colgate et al.[18] analyzed the problem of minimum energy required for ICF ignition by using a very simple model. While several refinements could be made to this model, we summarize only the most primitive form of this analysis. They reasonably equate the initial kinetic energy in the pusher to the sum of the internal energies in the D-T and the pusher at the time of maximum compression. This assumes that all the kinetic energy in the pusher is converted into internal energy. Colgate et al. also demand that the pressure times radius and the ignition temperature be reached at that time. Upon choosing an appropriate equation of state for the pusher (gamma law), they are able to derive an optimum pressure at ignition time that minimizes the energy required to achieve ignition. They were able to show that the minimum energy for ICF ignition depends on the inverse six to eighth power of implosion velocity (v^{-n}, where $n = 6$ to 8) and on the cube of the pressure times radius parameter *PR*. This prompts the question: Does the minimum energy for MTF ignition have the same scaling with velocity and the pressure times radius parameter that ICF does? If so, then because the value of *PR* required for MTF can be so small, but the velocity does not have to be very small, the energy required for MTF ignition might be exceedingly small.

For ICF, the minimum *PR* required for ignition is rather independent of the D-T mass in the target. In fact, it is taken as a constant in the analysis. As shown in Fig. 9, this is not the case for MTF. The size of the MTF region in the Lindl-Widner diagram depends on both the magnetic field *B* and the D-T mass. Note that the $B = 0$ dashed line represents the ICF case.

For D-T masses less than ~1 μg, the MTF region disappears for $B = 5$ MG. This sets an absolute minimum energy for a target that achieves a maximum field of 5 MG, that is, the energy necessary to provide the thermal energy in the D-T at the ignition temperature *T*. For $T = 10$ keV, the thermal energy of 1 μg is ~1 kJ. Of course, there is some energy left in the pusher at turnaround, so that the energy necessary to achieve ignition must be more. The aforementioned energy conservation analysis can be revised to consider the case of *PR* and the ignition temperature *T* being dependent on the D-T mass *m*. This results in the following relation for the implosion energy:

$$E = \frac{v^2}{v^2 - 2e_0[\langle PR\rangle^{3/2}/(mc_vT/2\pi)^{1/2}]^a}\, mc_vT \ . \quad (3)$$

Here, the minimum energy in the imploding target is found to depend on the implosion velocity v and the *PR*, but less strongly, and in a more complicated way than for the Colgate/Petschek analysis. The pusher equation of state enters this relation through the parameters $e_0 = P_0^{1/\gamma}/(\gamma - 1)\rho_0$ and $a = (\gamma - 1)/\gamma$. Rather than being a constant, *PR* now depends on the D-T mass, and for very large values of velocity or D-T mass, the necessary implosion energy is simply the thermal energy in the D-T. Figure 10 shows that for a given implosion velocity, there is an optimum D-T mass that minimizes the implosion energy needed for ignition.

From the information in Fig. 10, the locus of minimum energy as a function of implosion velocity for the optimum values of target mass can be derived. Figure 11 shows this locus, as well as the Colgate/Petschek

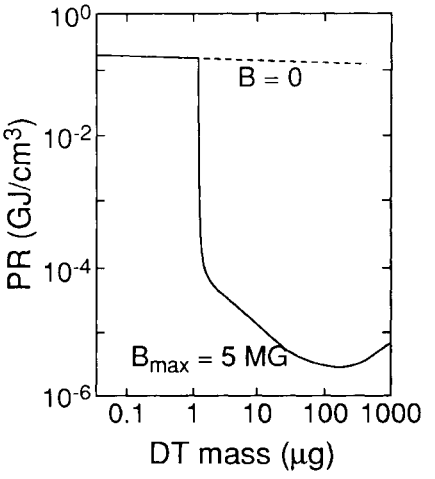

Fig. 9. Dependence of *PR* on D-T mass for $B = 0$ and for $B/\rho R = 10000$ and $B_{max} = 5$ MG.

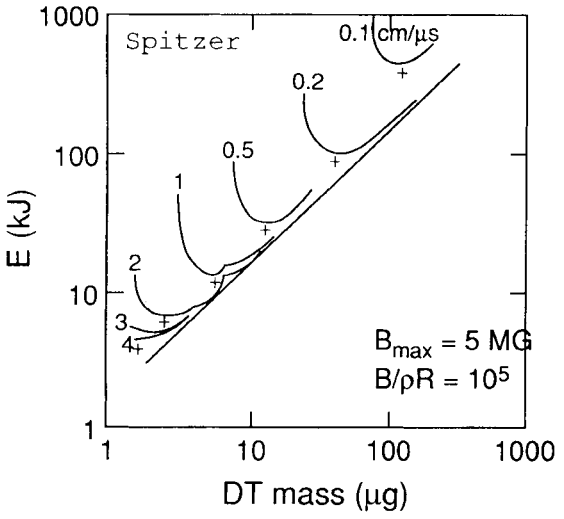

Fig. 10. The dependence of the minimum energy needed for ignition on the D-T mass.

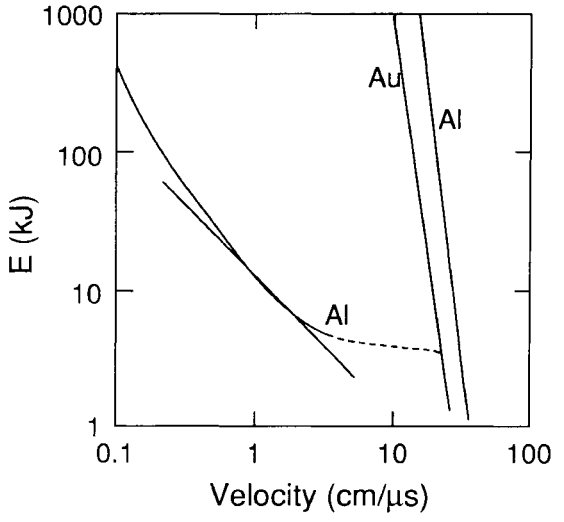

Fig. 11. The dependence of the minimum energy needed for ignition for an optimum target on the implosion velocity.

relation discussed earlier. For that $B = 0$ (ICF) case, there are two straight lines, one for each of two pusher materials, and the strong minimum energy dependence on the implosion velocity is apparent.

Figure 12 shows where MTF operates in the power and energy parameter space. Here the energy and power requirements for MTF are contrasted with those for ICF. While it is possible (according to the simple analysis cited earlier) to get ICF ignition at lower energies than for MTF, the power requirement is orders of magnitude greater. In terms of intensity on target, the difference is still more extreme. This extreme difference

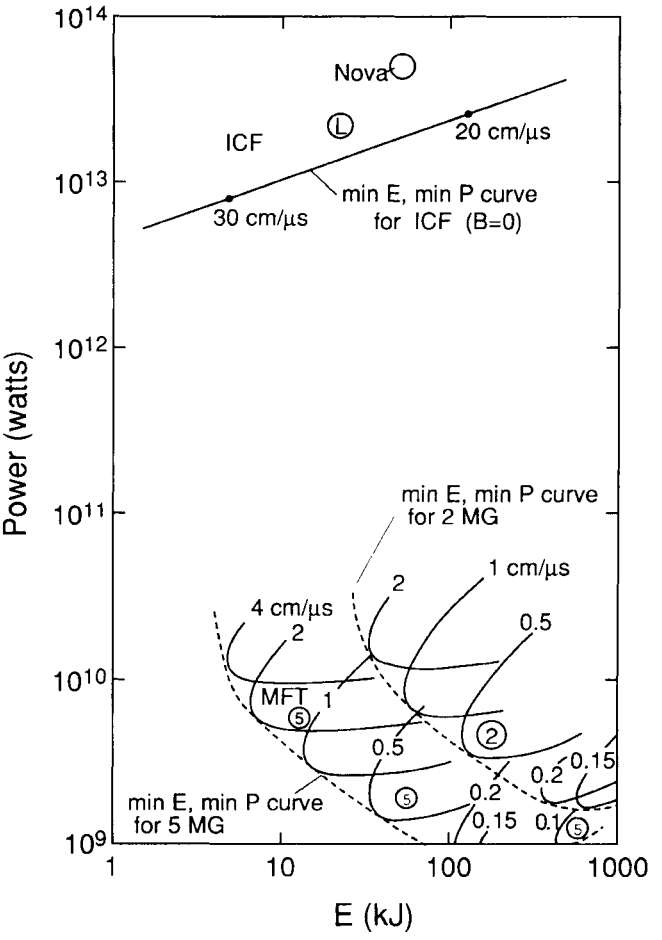

Fig. 12. The contrast between MTF and ICF in the power on target required for ignition. Note that the analysis presented here does not include considerations such as instabilities and plasma impurities.

between ICF and MTF has been previously illustrated through the use of initial condition phase-space,[4] where it was shown that there were separations that were orders of magnitude apart in the $Gain(\rho_0, v_0)$ phase-space.

XIII. POSSIBLE EXPERIMENTS

The most relevant experiments done to date are the Φ-targets, the Columbia University experiments, the fast liner experiments, the dense Z-pinch work, and the MAGO experiments in Russia. The Φ-targets were the only integral MTF experiments. The Columbia University experiments[9,10] measured the thermal conduction to the wall in a magnetized plasma produced by an electrically driven shock tube. These experiments should be repeated and extended.

Buiko et al. achieved 4×10^{13} D-T neutrons in their static MAGO experiments.[19] They used a slow

current source to establish a bias magnetic field in a low-density gas inside a cylindrical chamber with a metal barrier that divided the chamber into two parts connected along the cylindrical wall. This was followed by a fast discharge to create a reverse Z pinch, which forced the shock-heated plasma with the embedded bias field through the nozzle that connected the two parts. Upon shocking down in the second part of the chamber, significant heating occurred. These experiments have created a target plasma with the peak temperature exceeding 1 keV and a mean temperature calculated to be in the neighborhood of 160 eV. Buiko et al. stated that "Considering the (MAGO) chamber as thermonuclear target with preliminary heated DT-plasma, one may expect to achieve the ignition criterion when compressing the chamber by means of liner system" and that a substantial decrease in the required liner system compression velocity can be achieved (from 20 to 30 cm/μs down to 1 cm/μs) by employing preheating (and magnetization) of the D-T plasma.

Two lines of experimental effort could be pursued. One would be to repeat and extend the SNL Φ-target experiments with the better diagnostics and more energetic electron-beam machines available now. Another would be to marry the fast liner with a suitable target plasma. The liner implosion experiments in the fast liner program at LANL were a complete success, while the plasma preparation experiments had encouraging, but limited success. After that time, LANL has had significant success in producing kilovolt plasmas in high-density Z-pinch work done a few years ago.[20] The plasmas produced in those experiments were the result of a fast discharge through a frozen deuterium fiber. The fiber was pinched until it became unstable and exploded, thereby producing a hot, magnetized plasma. As the plasma expands toward the walls, it cools, but upon stagnation against the wall of the confining vessel, the energy of expansion (kinetic energy) should be converted back into internal energy to provide a hot, magnetized target plasma. The high-density Z pinch should be capable of providing an exceptionally clean and hot, magnetized plasma.[21]

XIV. CRITICAL ISSUES

The critical issues for MTF center around transport in the presence of a magnetic field, interaction of the plasma with the wall that supports and compresses it, plasma preparation, and engineering aspects.

The electron thermal conductivity is classically reduced as $1/[1 + (\omega\tau)^2]$, but Bohm diffusion only goes roughly as $1/\omega\tau$. While Bohm diffusion is a common process for magnetically confined fusion plasmas, it is not expected to be an important process for MTF because as we discussed earlier, the densities are much higher than for magnetically confined plasmas, making the ratio of plasma frequency to cyclotron frequency sufficiently high to destroy the plasma fluctuations that cause Bohm diffusion.

We believe that the SNL Φ-target experiments and the Columbia University experiments support an interpretation of classical reduction of thermal conduction by the magnetic field in the parameter space in which they operated. First, the two-dimensional MHD code[8] used to analyze one of the Φ-target experiments was based on the Braginskii equations,[22] which provide a classical reduction of electron thermal conductivity. The numerical results agreed with the experimental results for an assumed convergence of ~20. If Bohm-like diffusion had been operative or if other significant energy loss from the plasma had occurred, the plasma temperature would have additionally been suppressed so that a higher convergence would have been needed to match the experimental neutron yield. The neutron yield is very sensitive to temperature. Based on the calculations and other experience, one can see that the convergence being greater than 20 was unlikely. Second, the Columbia University experiments operated in a regime where the plasma-to-cyclotron frequency ratio is ~30 and the $\omega\tau$ is ~7, so that on the basis of theory concerning Bohm diffusion and particle simulations for dense plasmas,[17] one would expect classical reduction of electron thermal conductivity. Feinberg found that the measured flux in his experiment was about that predicted by classical theory.[10] This experimental confirmation of the theory for the plasma conditions studied (~10^6 cm^{-3}, 5 × 10^6 K, and 10 kG) is encouraging because MTF should operate in the high plasma-to-cyclotron frequency regime. However, there is still the possibility that under some conditions, Bohm-like diffusion might still operate. Mokhov asserted that MTF will work even if Bohm-like diffusion does apply,[23] but we have not yet examined his assertion or his reason for making it.

The charged alpha particles from the D-T fusion reaction are turned in the magnetic field. If BR exceeds ~0.3 MG·cm, the gyro radius is less than the target radius. While at low temperatures most of the energy of the alpha particles is deposited in the electrons, some is deposited in the ions, and these Rutherford collisions can have large scattering angles. This means that the path of the alpha particles will deviate from a simple trajectory (e.g., spirals in a uniform field) for slowing by electrons only.[24] The plasma ions throw a stochastic component into the trajectory that causes a random walk deviation from the electron-only path. To properly model this process, we may need to adapt the approach taken by Talley and Evans[25] for the unmagnetized case. They used Monte Carlo tracking of the reaction products and the secondary energy deposition by the knock-on plasma nuclei.

We do not consider physics of radiative losses to be a critical issue because we know and understand the radiative processes and the radiation transport problem for MTF. The important question concerns the level of

high-Z impurities that become entrained in the target plasma. One can take some precaution to minimize the level, such as using a low-Z pusher or a pusher lined with a low-Z material. Also, one would expect that a cold fuel layer would eliminate such a problem or reduce it from a radiative loss problem to one of increased heat capacity. Clearly, the question of impurity level is closely tied to the question of plasma/wall interaction.

Hydrodynamic instabilities are expected to play a less important role in MTF for two reasons. First, the target plasma conditions are not tied to a strong shock. A strong shock is necessary to set the initial conditions in the D-T for ICF so that the implosion proceeds along the correct thermodynamic trajectory (sometimes referred to as an adiabat). Because no strong shock is needed, it is possible to use a shockless acceleration of the pusher. This can possibly be accomplished with an electromagnetic implosion. Second, calculations show that during the early part of the implosion, the liner remains solid, so that material strength resists the growth of instabilities. The implosion velocities needed for MTF are low, and the pusher is more nearly incompressible, so that the inner interface is accelerated until near ignition time. While the density of the D-T is much lower for MTF, the Atwood number for Rayleigh-Taylor instability growth is only slightly closer to unity than for ICF, so one would expect similar Rayleigh-Taylor growth when the pusher decelerates. Kelvin-Helmholtz instability is most prominent for counterstreaming fluids of about the same density, so the Kelvin-Helmholtz instability growth for MTF should not be as important as for ICF. The perceived problem with Kelvin-Helmholtz instability is entrainment of pusher material in the fusion plasma, which would enhance radiative loss from the plasma. The development of Kelvin-Helmholtz depends on the flow of the plasma along the interface, and that flow is determined by the buoyancy of the high field regions in the plasma and the mass that must be accelerated to cause that flow. This is one of the reasons that a high-beta plasma is desirable for MTF. By high beta, we mean that the plasma (particle) pressure is much greater than the field pressure.

While some progress has been made on creating a target plasma similar to what appears to be necessary for MTF (both in the Φ-target experiments and the fast liner program), additional work seems necessary. The Russian MAGO results are very encouraging in this regard. However, we believe that the high-density Z pinch may provide an equally attractive target plasma. We still must demonstrate experimentally that a target plasma suitable for implosion can be created.

Because the convergence needed to achieve MTF ignition is only on the order of 10 to 15 (depending on the initial target plasma temperature), the demand for symmetry and machining accuracy is much less than for ICF. In addition, the targets are much larger, so that the relative tolerances are easier to satisfy. We have not explored the question of materials, but the pusher of the target only has to contain a gas under a modest pressure or even possibly a slight vacuum. One might speculate that the pusher could be dynamically formed from a hollow gas puff, or possibly made of frozen D-T, but practical considerations may preclude such a target.

As emphasized earlier, the chief advantage of MTF is that the driver can be orders of magnitude less powerful and intense than what is required for ICF. This means that a pulsed power machine should suffice as an MTF driver. In fact, two energy supplies are needed, the first to create the target plasma and the second to implode the target. Under ideal circumstances, each source must supply the requisite internal energy of the plasma plus whatever extra remains in the pusher and the driver (ideally 50% if perfect load matching is achieved). For MTF, the energy coupled to the D-T at ignition time appears to be a significantly higher fraction of the implosion energy than for ICF (50% for MTF compared with 20% for ICF). However, the ignition temperature for MTF is ~10 keV, compared to ~3 to 5 keV for ICF, so that the implosion energy needed for ignition is about the same for the same mass of D-T. For example, for a target containing 100 μg of D-T, ideally, 10 kJ should be needed for creation of the target plasma, and ~400 kJ should be needed for the implosion. The corresponding powers required should be 10 GW and 2 TW. If an ion or electron beam is used to implode the target, the intensity on target would be ~1 TW/cm^2. All this assumes that an implosion velocity of 1 cm/μs will suffice for ignition, and that hinges on the transport issues discussed at the outset of this section.

XV. SUMMARY

At this time, the most significant experimental activity in MTF is the MAGO experiments being conducted in Russia. Both theoretical and experimental work is needed. To do the experiments, we need to calculate a specific case, but to do honest calculations, we may have to add some physics to one of our MHD codes. While some one-dimensional calculations were done with the LASNEX code, the explicit algorithms in the code made it run very slowly. An implicit code seems essential for two-dimensional MTF calculations. The minimum mass that can be ignited for MTF is somewhat over 1 μg if the maximum achievable field is 5 MG. This sets a lower limit to the energy needed to achieve ignition for MTF. Potentially, there is a significant synergism between ICF and MTF, especially in the implosion physics. A wide range of pulsed power drivers should be applicable to MTF. If the physics is as favorable as it currently appears to be, then achievement of fusion ignition with the pulsed power driver technology available today should be possible.

ACKNOWLEDGMENTS

Some of the people at LANL who contributed to the material in this paper were P. Sheehey, F. Wysocki, D. Scudder, D. Winske, and J. Shlachter.

REFERENCES

1. R. LANDSHOFF, "Transport Phenomena in Completely Ionized Gas in the Presence of a Magnetic Field," LA-466, Los Alamos National Laboratory (1945); see also *Phys. Rev.*, **79**, 904 (1949).

2. M. M. WIDNER, "Neutron Production from Relativistic Electron Beam Targets," *Bull. Am. Phys. Soc.*, **22**, 1139 (1977).

3. S. Yu. GUSKOV, V. B. ROZANOV, and L. E. TREBULEVA, "Energy Transfer by Alpha Particles in a Laser Plasma Subjected to a Magnetic Field," *Sov. J. Quantum Electron.*, **8**, 1062 (1984).

4. I. R. LINDEMUTH and R. C. KIRKPATRICK, "Parameter Space for Magnetized Fuel Targets in Inertial Confinement Fusion," *Nucl. Fusion*, **23**, 263 (1983).

5. D. P. KILCREASE and R. C. KIRKPATRICK, "Magnetized Fuel Inertial Confinement Fusion," *Nucl. Fusion*, **28**, 1465 (1988).

6. M. A. SWEENY and A. V. FARNSWORTH, "High-Gain, Low-Intensity ICF Targets for a Charged-Particle Beam Fusion Driver," *Nucl. Fusion*, **21**, 41 (1981).

7. J. D. LINDL, "Physics of Ignition for ICF Capsules," *Proc. Int. School on Plasma Physics Course and Workshop Inertial Confinement Fusion*, Varenna, Italy, 1988, A. CARUSO and E. SINDONI, Eds., Societa Fisica.

8. I. R. LINDEMUTH and M. M. WIDNER, "Magnetohydrodynamic Behavior of Thermonuclear Fuel in a Preconditioned Electron Beam Imploded Target," *Phys. Fluids*, **24**, 753 (1981).

9. R. A. GROSS, "Physics of a Wall-Confined Fusion System," *Nucl. Fusion*, **15**, 729 (1975).

10. B. FEINBERG, "An Experimental Study of a Hot Plasma in Contact with a Cold Wall," *Plasma Phys.*, **18**, 265 (1976).

11. A. R. SHERWOOD et al., "Fast Liner Proposal," LA-6707-P, Los Alamos Scientific Laboratory (Aug. 1977).

12. R. A. GERWIN and R. C. MALONE, "Adiabatic Plasma Heating and Fusion-Energy Production by a Compressible Fast Liner," *Nucl. Fusion*, **19**, 155 (1979).

13. T. R. JARBOE, "Review of the Los Alamos Fast Liner Program," a presentation to group P-1 (1992).

14. I. I. GLASS and D. SAGLE, "Application of Explosive-Driven Implosions to Fusion," *Phys. Fluids*, **25**, 269 (1982).

15. R. C. KIRKPATRICK and I. R. LINDEMUTH, "Ignition and Burn in Inertially Confined Magnetized Fuel," *Fusion Technol.*, **20**, 834 (1991).

16. I. R. LINDEMUTH and R. C. KIRKPATRICK, "The Promise of Magnetized Fuel: High Gain in Inertial Confinement Fusion," *Fusion Technol.*, **20**, 829 (1991).

17. J. M. DAWSON, H. OKUDA, and B. ROSEN, "Collective Transport in Plasmas," *Methods Comput. Phys.*, **16**, 281 (1976).

18. S. A. COLGATE, A. G. PETSCHEK, and R. C. KIRKPATRICK, "Minimum Energy for Fusion Ignition, A Realistic Goal," LA-UR-92-2599, Los Alamos National Laboratory (1992).

19. A. M. BUIKO et al., "Investigations of Thermonuclear Magnetized Plasma Generation in the Magnetic Implosion System MAGO," *Physics of High Energy Densities*, MEGAGAUSS VI, Albuquerque, New Mexico (1992).

20. P. SHEEHEY, J. E. HAMMEL, I. R. LINDEMUTH, D. W. SCUDDER, J. S. SCHLACTER, R. H. LOVEBERG, and R. A. RILEY, Jr., "Two-Dimensional Direct Simulation of Deuterium-Fiber-Initiated Z Pinches with Detailed Comparison to Experiment," *Phys. Fluids*, **4**, 3698 (1992).

21. D. W. SCUDDER, J. S. SHLACHTER, J. E. HAMMEL, F. VENNERI, R. CHRIEN, R. LOVEBERG, and R. RILEY, "The Los Alamos Mega-Amp Fiber Z-Pinch Experiment," *Proc. Workshop Physics of Alternative Magnetic Confinement Schemes*, Varenna, Italy, 1990, p. 519, S. ORTOLANI and E. SINDONI, Eds., Societa Italiana di Fisica, Editrice Compositori, Bologna (1991).

22. S. I. BRAGINSKII, "Transport Processes in a Plasma," *Reviews of Plasma Physics*, Vol. 1, p. 205, M. A. LEONTOVICH, Ed., Consultants Bureau, New York (1965).

23. V. N. MOKHOV, All-Russian Institute for Experimental Physics (VNIIEF), Personal Communication (1992).

24. D. P. SMITHERMAN and R. C. KIRKPATRICK, "Energetic Alpha Particle Deposition in a Magnetized Plasma," *Fusion Technol.*, **20**, 838 (1991).

25. T. L. TALLEY and F. EVANS, "Monte Carlo Alpha Deposition," LA-UR-88-1698, Los Alamos National Laboratory (1988).

Ronald C. Kirkpatrick (BS, electrical engineering, 1959, and MS, physics, 1963, Texas A&M University; PhD, astronomy, University of Texas at Austin, 1969) is a staff member at Los Alamos National Laboratory.

Irvin R. Lindemuth (BS, electrical engineering, Lehigh University, 1965; MS, 1967, and PhD, 1971, applied science and engineering, University of California at Davis/Livermore) was a visiting professor in the Nuclear Engineering Department at Texas A&M University in 1991–1992 and remains a member of the graduate faculty as an adjunct professor.

Marjorie S. Ward (BS, physics, New Mexico Institute of Mining and Technology, 1993) is currently a graduate student in nuclear engineering at the University of Wisconsin.